The construction of homoclinic and heteroclinic orbitals in asymmetric strongly nonlinear systems based on the Padé approximant*

Feng Jing-Jing(冯晶晶)[a)b)c)], Zhang Qi-Chang(张琪昌)[a)b)c)†], and Wang Wei(王 炜)[a)b)c)]

[a)] *Department of Mechanics, School of Mechanical Engineering, Tianjin University, Tianjin* 300072, *China*

[b)] *Tianjin Key Labortory of Nonlinear Dynamics and Chaos Control, Tianjin University, Tianjin* 300072, *China*

[c)] *State Key Laboratory of Engines, Tianjin University, Tianjin* 300072, *China*

(Received 5 January 2011; revised manuscript received 16 May 2011)

In this paper, the extended Padé approximant is used to construct the homoclinic and the heteroclinic trajectories in nonlinear dynamical systems that are asymmetric at origin. Meanwhile, the conservative system, the autonomous system, and the nonautonomous system equations with quadratic and cubic nonlinearities are considered. The disturbance parameter ε is not limited to being small. The ranges of the values of the linear and the nonlinear term parameters, which are variables, can be determined when the boundary values are satisfied. New conditions for the potentiality and the convergence are posed to make it possible to solve the boundary-value problems formulated for the orbitals and to evaluate the initial amplitude values.

Keywords: bifurcation, Padé approximant, strongly nonlinearity, homoclinic and heteroclinic orbitals

PACS: 02.30.Hq, 47.20.Ky, 82.40.Bj **DOI:** 10.1088/1674-1056/20/9/090202

1. Introduction

The formation of the homoclinic and the heteroclinic orbitals is taken as one of the criteria for the transition from regular to chaotic behaviour in solutions of a dynamical system.[1−5] The study of the homoclinic and the heteroclinic bifurcations[6−8] in a nonlinear dynamic system has great theoretical value to the analysis of the global behaviour of that system. The available analytical methods for studying the homoclinic and the heteroclinic bifurcations, e.g., the well-known Melnikov method,[9] have universal problems such as limited application and short precision. It is necessary to improve the existing analytical methods to study the global dynamic behaviour of nonlinear systems.

In the construction of the homoclinic and the heteroclinic orbitals for nonlinear dynamical systems, numerical simulations are used in most cases. In contrast analytical approaches are rarely used. The Padé approximants (PA) were successfully used for the homoclinic orbitals of two-dimensional axisymmetric breathers by Vakakis.[10] The quasi-Padé approximants (QPA) were used to construct the homoclinic orbitals in a nonlinear Schrodinger equation system by Mikhlin.[11] The analytic homoclinic orbitals in the nonautonomous Duffing equation and in the Van der Pol–Duffing equation with weakly coupled nonlinear oscillators were computed in Ref. [12]. Zhang *et al.*[13,14] used the extended normal form method to analyze the homoclinic and the heteroclinic bifurcations of a strongly nonlinear oscillator. Recently Chen *et al.*[15,16] used the hyperbolic perturbation method to determine the homoclinic solution of certain strongly quadratic nonlinear autonomous oscillators. However, an effective analytic approximation of the heteroclinic orbitals is difficult and has not been solved so far, so is the homoclinic orbitals in the asymmetric system at origin.

In this paper, we use the extended PA to generate solutions that satisfy the boundary value of the homoclinic and the heteroclinic solutions and then derive the critical values of the bifurcations in the corresponding conservative, autonomous, and nonautonomous systems with quadratic and cubic nonlinear oscillators, in which the parameters of the linear and the nonlinear terms are variable. The comparison of the analytical orbitals with variable parameters de-

*Project supported by the National Natural Science Foundation of China (Grant Nos. 11072168 and 10872141).

†Corresponding author. E-mail: qzhang@tju.edu.cn

© 2011 Chinese Physical Society and IOP Publishing Ltd

rived in our approach with the results of numerical simulations confirms that the accuracy of the solutions is improved significantly when the extended approach is used to analyze the problem of the analytical homoclinic and heteroclinic orbitals in the strongly asymmetric nonlinear systems.

2. Conservative systems

Consider equation

$$\ddot{x} + c_1 x + \varepsilon(c_2 x^2 + c_3 x^3) = 0 \tag{1}$$

where c_1, c_2, c_3, and ε are arbitrary, and ε is the perturbation parameter. A separatrix of the equation, which is a solution satisfying the special boundary value, will be constructed using the PA.[17,18]

Firstly, the property of the conservative system (1) needs to be analyzed. The integral of Eq. (1) is

$$\frac{1}{2}\dot{x}^2 + V(x) = E, \tag{2}$$

where $\dot{x}^2/2$ is the kinetic energy, $V(x)$ is the potential energy, and E is the total energy of the system. Particularly,

$$\begin{aligned} V(x) &= \int_0^x [c_1 x + \varepsilon(c_2 x^2 + c_3 x^3)]\,\mathrm{d}x \\ &= \frac{1}{2}c_1 x^2 + \varepsilon\left(\frac{1}{3}c_2 x^3 + \frac{1}{4}c_3 x^4\right). \end{aligned} \tag{3}$$

So, the series solution of Eq. (1) is

$$x(t) = a_0 + a_1 t + \cdots = \sum_{n=0}^{\infty} a_n t^n, \tag{4}$$

where point (a_0, a_1) is the initial values of the trajectories

$$x(0) = a_0, \quad \dot{x}(0) = a_1. \tag{5}$$

Parameters a_0 and a_1 are arbitrary constants and cannot be zero simultaneously. The other parameters can be expressed as algebraic polynomials through a_0, a_1, c_1, c_2, c_3, ε,

$$a_2 = \frac{1}{2}(-a_0 c_1 - \varepsilon a_0^2 c_2 - \varepsilon a_0^3 c_3), \tag{6}$$

$$a_3 = -\frac{1}{6}a_1(c_1 + 2\varepsilon a_0 c_2 + 3\varepsilon a_0^2 c_3), \tag{7}$$

$$\begin{aligned} a_4 = \frac{1}{24}(&a_0 c_1^2 - 2\varepsilon a_1^2 c_2 + 3\varepsilon a_0^2 c_1 c_2 \\ &+ 2\varepsilon^2 a_0^3 c_2^2 - 6\varepsilon a_0 a_1^2 c_3 + 4\varepsilon a_0^3 c_1 c_3 \\ &+ 5\varepsilon^2 a_0^4 c_2 c_3 + 3\varepsilon^2 a_0^5 c_3^2), \\ &\cdots . \end{aligned} \tag{8}$$

2.1. When $c_1 < 0$, $c_3 > 0$, $c_2 = 0$

System (1) satisfies the conditions

$$\dot{x}(0) = 0, \quad \lim_{t\to\infty} x(t) = 0.$$

In this case, the initial value is $(a, 0)$,

$$a_0 = a, \quad a_1 = 0. \tag{9}$$

The a, which is the point of the intersection between the homoclinic orbitals and the x axis, is the extreme value point. The coefficients given in Eqs. (6)–(8) can be expressed through algebraic polynomials as

$$a_{2n+1} = 0, \quad a_{2n} = P_{2n}(a), \quad (n \geq 0).$$

All the coefficients of PA_4 are obtained by comparing PA_4 with the Taylor expansion of the solution, namely,

$$\sum_{n=0}^{\infty} a_{2n} t^{2n} \cong \mathrm{PA}_4. \tag{10}$$

We obtain nine equations, which are Eqs. (A1)–(A6) in the appendix.

Consider the convergence condition[19]

$$\Delta_4 = 0, \tag{11}$$

c_1 and c_3 can be chosen arbitrarily. Taking $c_1 = -1$ and $c_3 = 2$ as an example, when $\varepsilon = 500$ the initial value of a is obtained as $a = 0.0446956$, and the error between the above value and $a = 1/10\sqrt{5}$ is less than 0.05753%. The homoclinic solution is given in the form

$$\mathrm{PA}_4 = \frac{0.0446956 - 0.00202178t^2 + 0.0000500014t^4}{1 + 0.453615t^2 + 0.0198375t^4}. \tag{12}$$

The other initial value is equal to it but opposite in sign; the homoclinic orbital and the orbital mentioned above are symmetric with respect to the origin.

In contrast to the result of the numerical simulation, for nonlinear systems with weak or strong nonlinearity, i.e. $\varepsilon = 0.1$, 1, 500, our method always gives a good prediction, which is shown in Fig. 1. It also confirms that the solution is accurate, because the dotted line almost coincides with the solid line.

Then in combination with other approximants, the coefficients of the homoclinic solution PA in the conservative Duffing system are

$$\alpha_{2n+1} = 0, \quad \beta_{2n+1} = 0, \quad n = 0, 1, 2, \ldots \tag{13}$$

And the homoclinic solution PA can be obtained as

$$\mathrm{PA}_n = \frac{\sum_{k=0}^{n} \alpha_{2k} t^{2k}}{1 + \sum_{k=1}^{n} \beta_{2k} t^{2k}}. \tag{14}$$

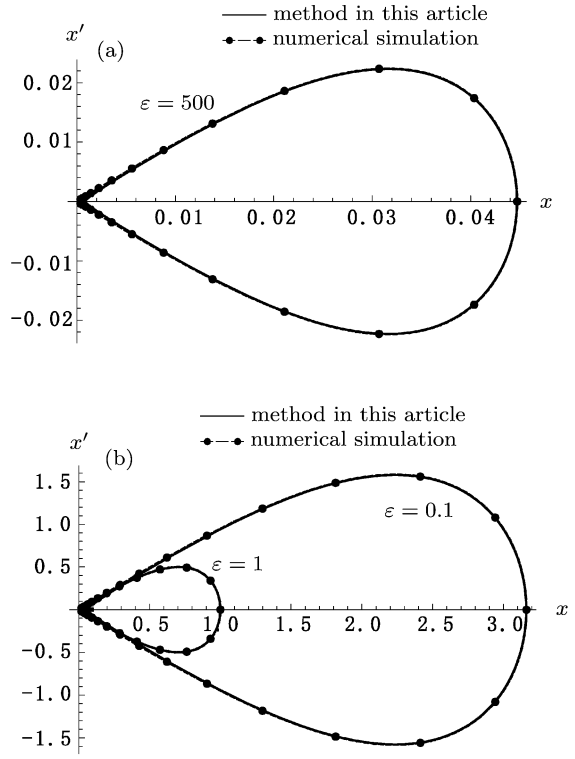


Fig. 1. Comparison of homoclinic trajectories obtained using the present results with those obtained in the Runge–Kutta procedure for (a) $\varepsilon = 500$, (b) $\varepsilon = 0.1$, and $\varepsilon = 1$.

2.2. When $c_1 > 0$, $c_3 < 0$, $c_2 = 0$

System (1) satisfies the conditions

$$\lim_{t\to\pm\infty} x(t) = \pm\sqrt{-c_1/c_3}, \lim_{t\to\pm\infty} \dot{x}(t) = 0$$

or

$$\lim_{t\to\pm\infty} x(t) = \mp\sqrt{-c_1/c_3}, \lim_{t\to\pm\infty} \dot{x}(t) = 0.$$

Suppose the initial value is $(0, b)$,

$$a_0 = 0, \quad a_1 = b. \tag{15}$$

The b, which is the point of the intersection between the heteroclinic orbitals and the y axis, is the extreme value point. The process of computation is similar to the previous one. The coefficients can be expressed through algebraic polynomials as

$$a_{2n} = 0, \quad a_{2n+1} = P(b), \quad (n \geq 0).$$

The c_1 and c_3 can be chosen arbitrarily. Taking $c_1 = 1$ and $c_3 = -1$ as an example, when $\varepsilon = 500$, the initial value of b is obtained as $b = 0.0316226$, and the error between the above value and the result of the numerical simulation $b = 0.0316227$ is less than 0.000316229%. The heteroclinic solution is

$$\mathrm{PA}_6 = \frac{0.0316226t + 0.00192847t^3 + 0.0000165554t^5}{1 + 0.227651t^2 + 0.00513224t^4 + 0.0000130431t^6}. \tag{16}$$

The other initial value has an equal absolute value with the one shown above but is opposite in sign; the other half of the heteroclinic orbital and the orbital mentioned above are symmetric with respect to the origin.

Figure 2 shows the comparison of the orbitals constructed using the Runge–Kutta procedure with those constructed using the PA.

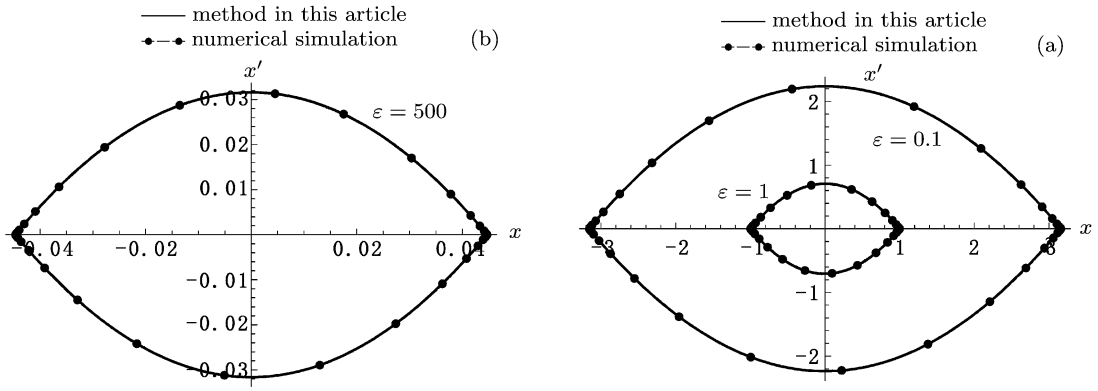


Fig. 2. Comparison of heteroclinic trajectories obtained using the present results with those obtained using the Runge–Kutta procedure for (a) $\varepsilon = 500$, (b) $\varepsilon = 0.1$, and (c) $\varepsilon = 1$.

The heteroclinic solution PA and its coefficients are

$$\alpha_{2n} = 0, \quad \beta_{2n+1} = 0, \quad n = 0, 1, 2, \ldots, \tag{17}$$

$$\mathrm{PA}_n = \frac{\sum_{k=0}^{n} \alpha_{2k+1} t^{2k+1}}{1 + \sum_{k=1}^{n} \beta_{2k} t^{2k}}. \tag{18}$$

2.3. When $c_2^2 > 4c_1c_3$, $c_2c_3 \neq 0$, $c_1 < 0$

System (1) satisfies the conditions

$$\dot{x}(0) = 0, \quad \lim_{t\to\infty} x(t) = 0.$$

The potential energy curves and the phase portraits of system (1) with $c_2c_3 < 0$ and $c_2c_3 > 0$ are shown in Fig. 3. In the phase space, there are two homoclinic orbitals Γ_1 and Γ_2, which are symmetric with respect to the x axis but not to the $\dot{x}$ axis. The common saddle point H that they share is at $(0,0)$ and the two centres are at $O_1(-\frac{1}{2c_3}[c_2+\sqrt{c_2^2-4c_1c_3}],0)$ and $O_2(-\frac{1}{2c_3}[c_2-\sqrt{c_2^2-4c_1c_3}],0)$ respectively. The phase points on the two homoclinic orbitals approach the saddle point H along $A_1B_1D_1$ and $A_2B_2D_2$ when $t \to +\infty$. When $t \to -\infty$, the phase points approach the same saddle point H along the reverse directions. That is the homoclinic nature of homoclinic orbitals Γ_1 and Γ_2. Thus, the homoclinic solutions satisfy the conditions

$$\lim_{t\to\pm\infty} x = 0, \quad \lim_{t\to\pm\infty} \dot{x} = 0 \tag{19}$$

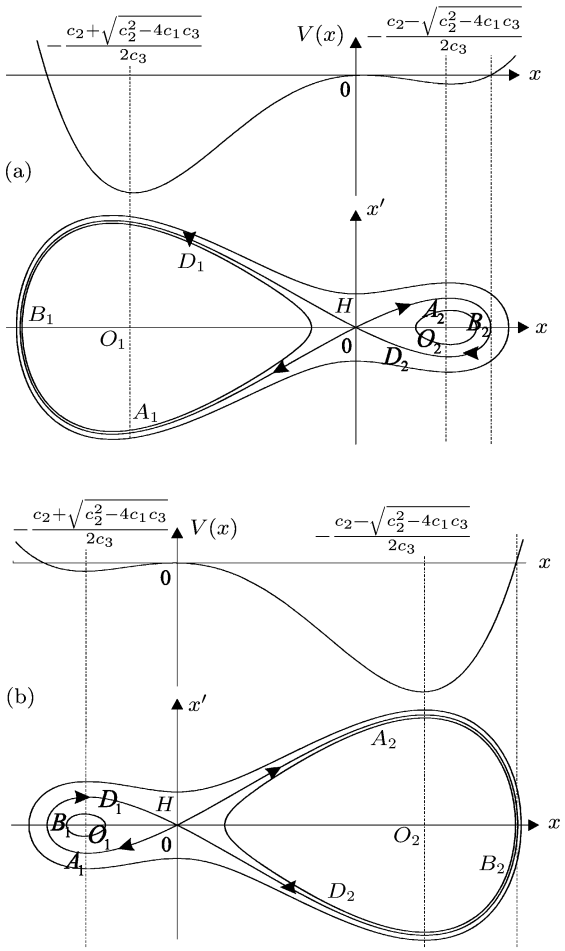


Fig. 3. Potential energy curves and phase diagrams for Eq. (7) with (a) $c_2c_3 > 0$ and (b) $c_2c_3 < 0$.

Let the initial value be $(a, 0)$,

$$a_0 = a, \quad a_1 = 0. \tag{20}$$

The a, which is the point of the intersection between the homoclinic orbitals and the x axis, is the extreme value point. The coefficients of series solution $x(t)$ satisfy the property

$$a_{2n+1} = 0, \quad a_{2n} = P_{2n}(a), \quad (n \geq 0).$$

We consider the convergence condition based on the homoclinic nature. Let the limit PA be the saddle point,

$$\mathrm{PA}_n \to 0. \tag{21}$$

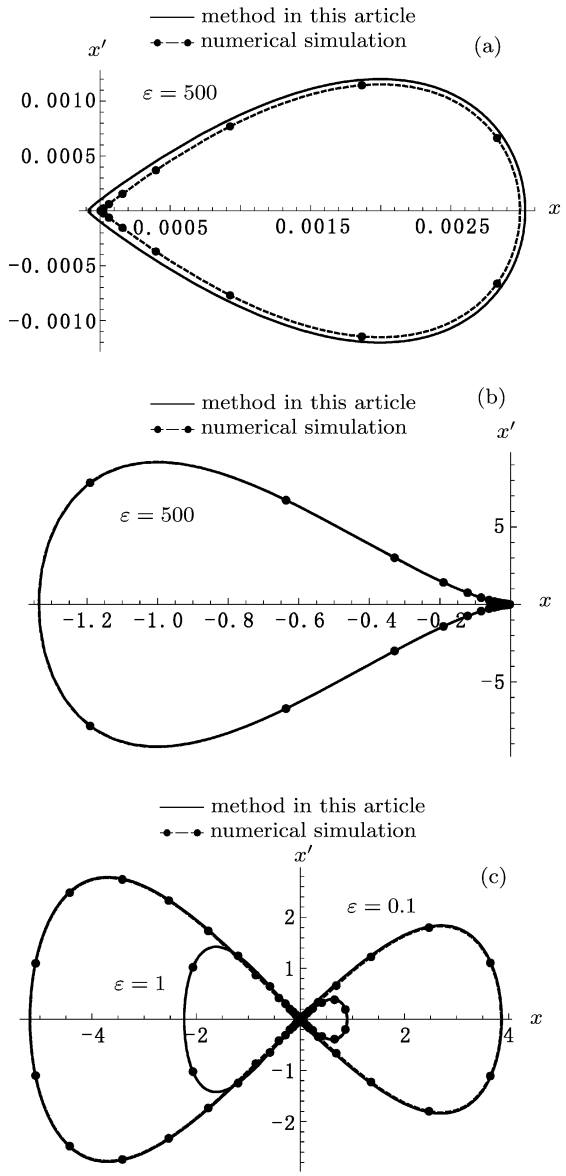


Fig. 4. Comparison of the homoclinic trajectory obtained using the present results with those obtained in the Runge–Kutta procedure for (a) the right-hand side of $\varepsilon = 500$, (b) the left-hand side of $\varepsilon = 500$, and (c) $\varepsilon = 0.1$ and $\varepsilon = 1$.

The c_1, c_2, and c_3 can be chosen arbitrarily. Here we take $c_1 = -1$, $c_2 = 1$, and $c_3 = 1$ as Example 1 to obtain a fourth-order approximation solution. When $\varepsilon = 500$, the initial value of a is obtained as $a = 0.00303033$, and the error between the above value and the result of the numerical simulation $a = 3/[5(100 + \sqrt{10090})]$ is less than 0.000399202%. The homoclinic solution is

$$\mathrm{PA}_4^+ = \frac{0.00303033 - 0.000130353t^2}{1 + 0.216862t^2 + 0.0120896t^4}. \quad (22)$$

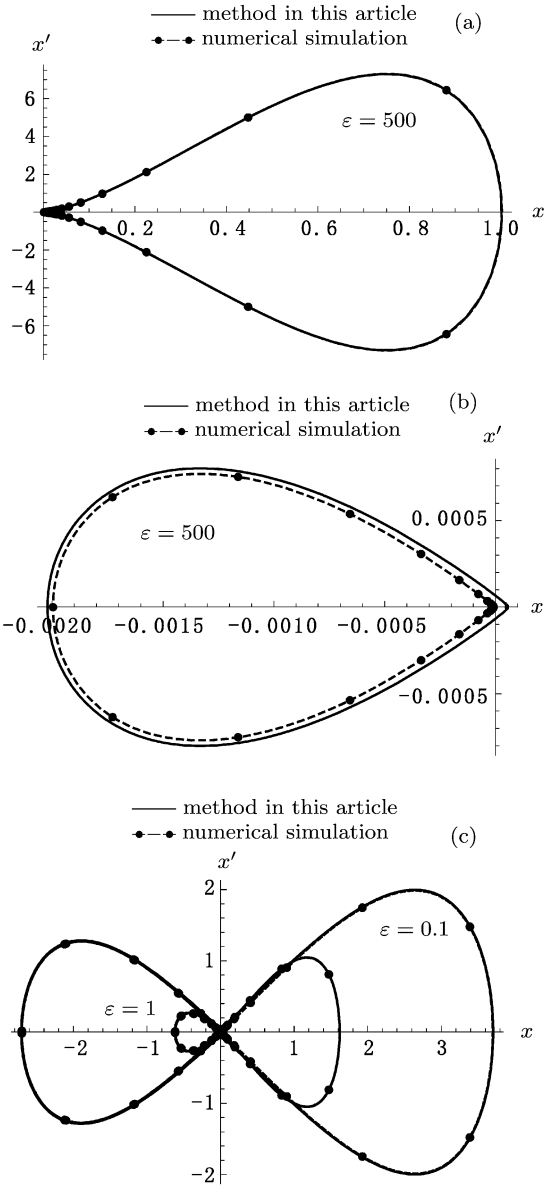


Fig. 5. Comparison of homoclinic trajectories obtained using the present results with those obtained in the Runge–Kutta procedure for (a) the right-hand side of $\varepsilon = 500$, (b) the left-hand side of $\varepsilon = 500$, and (c) $\varepsilon = 0.1$ and $\varepsilon = 1$.

The other initial value is $a = -1.33673$, and the error is less than 0.482769%. The corresponding homoclinic solution is

$$\mathrm{PA}_4^- = \frac{-1.33633 + 0.0445864t^2}{1 + 111.827t^2 + 5.58951t^4}. \quad (23)$$

In contrast to the result of the numerical simulation, this gives a good prediction, as shown in Fig. 4.

We take $c_1 = -1$, $c_2 = -1.5$, and $c_3 = 2$ as Example 2. In this case, when $\varepsilon = 500$, the initial value $a = 1.001996$ can be obtained. The error between the above value and the result of the numerical simulation $a = 1.002$ is less than 0.000399202%. The homoclinic solution is

$$\mathrm{PA}_4^+ = \frac{1.002 - 0.0333447t^2 - 0.0000295391t^4}{1 + 125.716t^2 + 6.29438t^4}. \quad (24)$$

The other initial value is $a = -0.00202074$, and the error is less than 0.502691%. The homoclinic solution is

$$\mathrm{PA}_4^- = \frac{-0.00202074 + 0.0000869293t^2}{1 + 0.2168t^2 + 0.0120869t^4}. \quad (25)$$

Figure 5 shows the comparison of the orbitals constructed using the Runge–Kutta procedure with those constructed using the PA.

The QPA and the PA are not effective at computing the homoclinic solution of a conservative system with the quadratic and the cubic nonlinear oscillators. Figure 5 shows that the error between the results generated by the analytic solution and by the numerical simulation is small when the extended PA is used.

3. Value of global bifurcation

Considering the autonomous system with quadratic and cubic nonlinear oscillators,

$$\ddot{x} + c_1 x + \varepsilon(c_2 x^2 + c_3 x^3) = \varepsilon f(\mu, x, \dot{x}). \quad (26)$$

Letting $\varepsilon = 0$, the conservative system of Eq. (26) is obtained,

$$\ddot{x} + c_1 x + \varepsilon(c_2 x^2 + c_3 x^3) = 0, \quad (27)$$

which is the same as Eq. (1). By employing the expression of the homoclinic orbitals at time t in the conservative system, the expression for the well-known Melnikov function can be written as

$$\int_{-\infty}^{+\infty} \dot{x}_0 f(\mu, x, \dot{x}) \mathrm{d}t = 0, \quad (28)$$

where

$$x_0(t) = \mathrm{PA}_n, \quad \dot{x}_0(t) = \frac{\mathrm{d}}{\mathrm{d}t}(\mathrm{PA}_n). \quad (29)$$

The specific form is determined by the cases discussed in Section 2. When the homoclinic bifurcations occur in system (26), equation (28) is satisfied, and bifurcation value μ can be calculated based on Eq. (28).

The disturbance can be freely selected. Now we consider the system

$$\ddot{x} + c_1 x + \varepsilon(c_2 x^2 + c_3 x^3) = \varepsilon(\mu + \mu_1 x - \mu_2 x^2)\dot{x}, \quad (30)$$

namely,

$$f(\mu, x_0, \dot{x}_0) = \varepsilon(\mu + \mu_1 x - \mu_2 x^2)\dot{x},$$

where μ is the control parameter, and μ_1 and μ_2 are constants. We assume the following condition is established,

$$I(t) = \int \dot{x}_0 f(\mu, x_0, \dot{x}_0)\,\mathrm{d}t = \int (\mu + \mu_1 x_0 - \mu_2 x_0^2)\dot{x}_0\,\mathrm{d}t. \quad (31)$$

The c_1, c_2, c_3, μ_1, and μ_2 can be chosen arbitrarily. In Eq. (27), we assign them to the same values as they were in the previous example. Substitute $x_0(t) = \mathrm{PA}_n$ which is derived from the specific expression of the homoclinic or the heteroclinic solution mentioned above into the second equation of Eq. (29) and then put them into Eq. (31). By means of simplification and integration, the globe bifurcation is obtained. Table 1 lists the results of the three cases. In case 3, the left and the right orbitals are employed respectively, because the orbitals are not symmetric with respect to the origin.

Table 1. Comparison of the present results with the numerical simulation.

	$c_1 < 0$, $c_3 > 0$, $c_2 = 0$	$c_1 > 0$, $c_3 < 0$, $c_2 = 0$	$c_2^2 < 4c_1c_3$, $c_2c_3 \neq 0$, $c_1 < 0$	
$x_0(t)$	Eq. (12)	Eq. (16)	Eq. (22)	Eq. (23)
μ_1	0	0	1	1
μ_2	1	–1	1	1
ε	500	500	500	500
μ_c	0.000802403	–0.000399755	1.61561	–0.0016878
Numerical simulation	0.000797631	–0.000399981	1.61671	–0.0017073

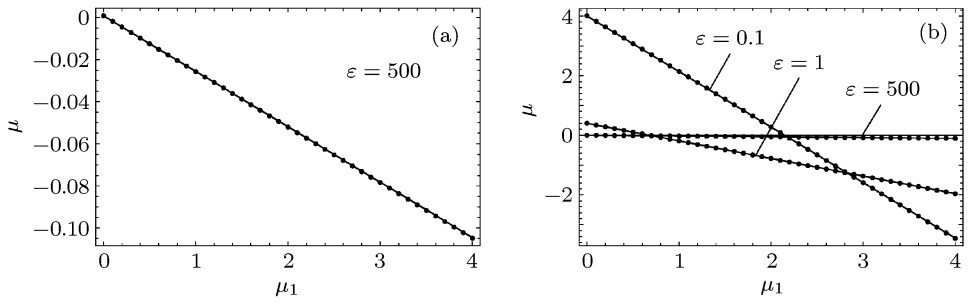


Fig. 6. Boundaries of homoclinic bifurcation in parameter space (μ, μ_1) of the autonomous system (30) obtained by our proposed method and by the numerical simulation when $\mu_2 = 1$: (a) partial enlarged plot of $\varepsilon = 500$, (b) $\varepsilon = 0.1$, $\varepsilon = 1$, and $\varepsilon = 500$.

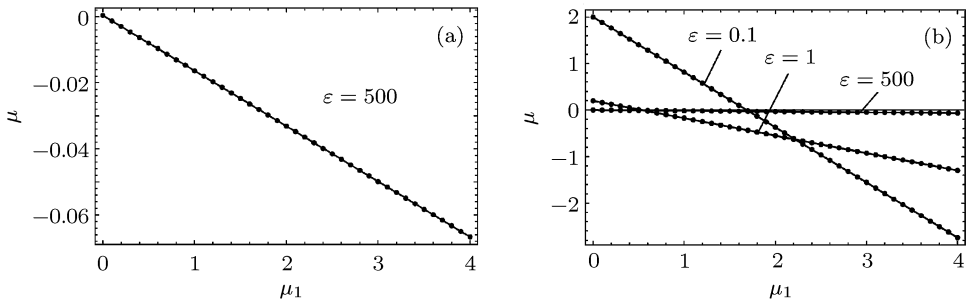


Fig. 7. The boundaries of heteroclinic bifurcation in parameter space (μ, μ_1) of the autonomous system (30) obtained by our proposed method and by the numerical simulation when $\mu_2 = 1$; (a) partial enlarged plot of $\varepsilon = 500$, (b) $\varepsilon = 0.1$, $\varepsilon = 1$, and $\varepsilon = 500$.

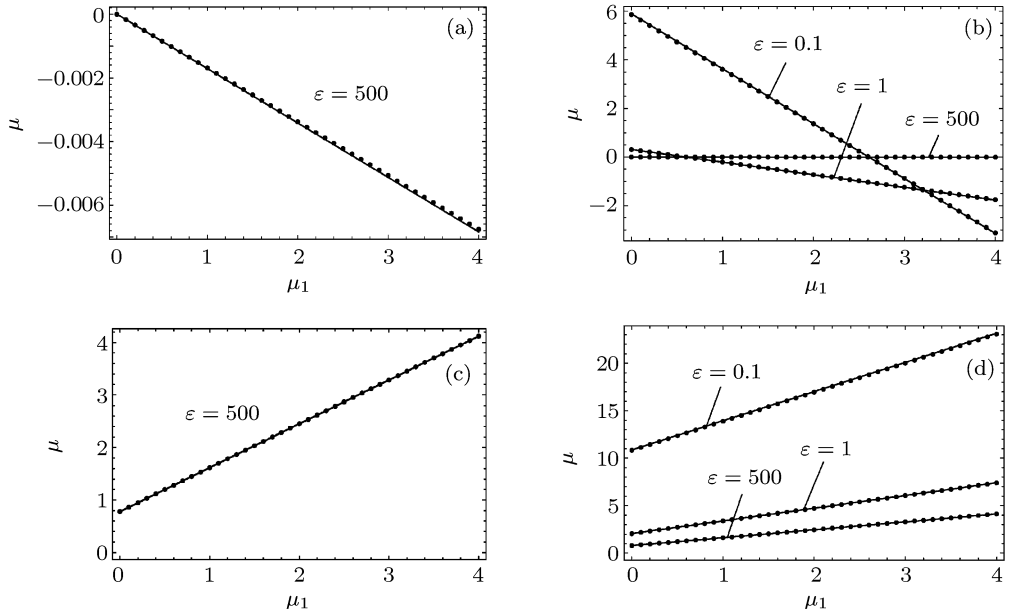


Fig. 8. The boundaries of homoclinic bifurcation in parameter space (μ, μ_1) of autonomous asymmetric system (30) obtained by our proposed method and by the numerical simulation when $\mu_2 = 1$: (a) partial enlarged drawing of $\varepsilon = 500$ on the right-hand side, (b) $\varepsilon = 0.1$, $\varepsilon = 1$, and $\varepsilon = 500$ on the right-hand side, (c) partial enlarged drawing of $\varepsilon = 500$ on the left-hand side, (d) $\varepsilon = 0.1$, $\varepsilon = 1$, and $\varepsilon = 500$ on the left-hand side.

We fix parameter $\mu_2 = 1$, let frequency μ_1 vary in the range $(0, 4)$, and then calculate the homoclinic or the heteroclinic bifurcations. The left-hand side and the right-hand side critical homoclinic bifurcation values of the asymmetric system are calculated respectively. The boundaries of the homoclinic or the heteroclinic bifurcations in parameter place (μ, μ_1) obtained by our proposed method (dotted line) and by the numerical simulation (solid line) are shown in Figs. 6–8. We note that the initial values and the change rate of μ_1 decrease as ε increases.

4. Potentiality condition

The PA is extended by us to study the nonlinear differential equations. First of all, it is an efficient and rational approximation, which is not necessarily limited by the range of ε when the method is applied to solve the nonlinear differential equations. Therefore, the method can be applied not only to the weakly nonlinear systems but also to the strongly nonlinear ones. Secondly, the solution obtained by our method has a simple form, which can be directly expressed as a function of time t. It is fundamentally important to the following work, such as the analysis of the nature of the solution.

Now the extended PA is used to study the autonomous system. When $\varepsilon = 0$, the general expressions of the homoclinic and the heteroclinic solutions in the conservative system can be expressed as Eqs. (14) and (18), respectively. When $\varepsilon \neq 0$, the expressions of the homoclinic and the heteroclinic solutions in the autonomous system are similar to those of the conservative system. That is

$$x(t) = \mathrm{PA}_n = \frac{\sum\limits_{k=0}^{n} \alpha_k t^k}{1 + \sum\limits_{k=1}^{n} \beta_k t^k}$$

or

$$\mathrm{PA}_n = \frac{\sum\limits_{k=0}^{n} \alpha_{2k+1} t^{2k+1}}{1 + \sum\limits_{k=1}^{n} \beta_{2k} t^{2k}}.$$

The traditional perturbation method usually assumes the solution as a power function expressed using ε. If the perturbation parameter ε is not small enough, such as ε in the strongly nonlinear system, the calculation is not valid. With the new method, the differential equation including ε is solved directly. It can maintain the accuracy of the traditional method, namely, the high order items can be ignored when ε is small enough. And, if ε is not small enough, the new method can also be used. It extends the range of calculation and accuracy.

In the conservative system, the extreme value points on the x or the y axis can be chosen based

on the characteristics of the system. Meanwhile, after a disturbance, the extreme value points in the origin system may have some small changes, and then the locations of the original chosen points would not be certain. It is proved that the disturbance has influence on the location and the nature of the initial point in the conservative system.

In the perturbation, we assume that the homoclinic orbital has been deformed but does not break down, namely, the extreme value point is no longer to be the intersection between the orbital and the x axis. Now let us assume the initial point to be the extreme value point of the orbital, which locates at (a_0, a_1), and its tangent is perpendicular to the x axis. The solutions satisfy the following condition,

$$\left.\frac{\mathrm{d}x(t)}{\mathrm{d}y(t)}\right|_{t=0} = 0,$$

where

$$y(t) = \frac{\mathrm{d}x(t)}{\mathrm{d}t} = \dot{x}(t).$$

Then,

$$\left.\frac{\mathrm{d}x(t)}{\mathrm{d}y(t)}\right|_{t=0} = \left.\frac{\mathrm{d}x(t)}{\mathrm{d}\dot{x}(t)}\right|_{t=0} = \left.\frac{\dfrac{\mathrm{d}x(t)}{\mathrm{d}t}}{\dfrac{\mathrm{d}\dot{x}(t)}{\mathrm{d}t}}\right|_{t=0} = \left.\frac{\dot{x}(t)}{\ddot{x}(t)}\right|_{t=0} = 0,$$

that is,

$$\dot{x}(0) = 0, \quad \ddot{x}(0) \neq 0,$$

namely,

$$a_1 = 0, \quad a_2 \neq 0. \tag{32}$$

This contradicts with the assumption. So the extreme value point in the initial time is still the intersection between the orbital and the x axis.

In the calculation of the heteroclinic orbital, the initial point located at (a_0, a_1) has a tangent that is perpendicular to the y axis. The process of the calculation is similar to the previous one. The extreme value point selected at the initial time is no longer to be the intersection between the orbital and the y axis, but is the point satisfying the conditions

$$a_2 = 0, \quad a_1 \neq 0. \tag{33}$$

5. Autonomous system

Here we still consider the van der Pol oscillators,

$$\ddot{x} + c_1 x + \varepsilon(c_2 x^2 + c_3 x^3) = \varepsilon(\mu + \mu_1 x - \mu_2 x^2)\dot{x}. \tag{34}$$

The series solution of autonomous Eq. (34) can be expressed in the form

$$x(t) = a_0 + a_1 t + \cdots = \sum_{n=0}^{\infty} a_n t^n, \tag{35}$$

where point (a_0, a_1) is the initial value of the trajectories. Parameters a_0 and a_1 are arbitrary constants and cannot be equal to zero simultaneously. We consider the effect of the disturbance parameters directly. The other parameters can be expressed as algebraic polynomials through a_0, a_1, c_1, c_2, c_3, ε, μ, μ_1, and μ_2,

$$\begin{aligned} a_2 = {} & \frac{1}{2}(\mu\varepsilon a_1 - a_0 c_1 - \varepsilon a_0^2 c_2 - \varepsilon a_0^3 c_3 \\ & + \varepsilon a_0 a_1 \mu_1 - \varepsilon a_0^2 a_1 \mu_2), \end{aligned} \tag{36}$$

$$\begin{aligned} a_3 = {} & \frac{1}{6}(2\mu\varepsilon a_2 - 2\varepsilon a_0 a_1 c_2 - 3\varepsilon a_0^2 a_1 c_3 + \varepsilon a_1^2 \mu_1 \\ & - 2\varepsilon a_0 a_2 \mu_1 - 2\varepsilon a_0 a_1^2 \mu_2 \\ & - 2\varepsilon a_0^2 a_2 \mu_2 - a_1 c_1), \end{aligned} \tag{37}$$

$$\begin{aligned} a_4 = {} & \frac{1}{12}(3\mu\varepsilon a_3 - a_2 c_1 - \varepsilon a_1^2 c_2 - 2\varepsilon a_0 a_2 c_2 \\ & - 3\varepsilon a_0 a_1^2 c_3 - 3\varepsilon a_0^2 a_2 c_3 + 3\varepsilon a_1 a_2 \mu_1 + 3\varepsilon a_0 a_3 \mu_1 \\ & - \varepsilon a_1^3 \mu_2 - 6\varepsilon a_0 a_1 a_2 \mu_2 - 3\varepsilon a_0^3 a_3 \mu_2), \end{aligned} \tag{38}$$

$$\cdots .$$

The value of the global bifurcation has been computed in Section 4, and now we give the conclusion directly

Table 2. All parameters involved in the calculation of the three cases.

Case	$c_1 < 0$, $c_3 > 0$, $c_2 = 0$	$c_1 > 0$, $c_3 < 0$, $c_2 = 0$	$c_2^2 < 4c_1c_3$, $c_2c_3 \neq 0$, $c_1 < 0$
Solution	homoclinic	heteroclinic	homoclinic
Initial point	$(a, 0)$	(a, a_1)	$(a, 0)$
ε	500	500	500
μ_c	0.000802403	–0.000399755	–0.00168783
a	0.0434771	–0.00499391	0.00303072
Asymmetric	yes	yes	no

Similar to the conservative system (1), the autonomous system (34) is discussed in the three cases. Table 2 lists all the parameters involved in the calculation of these three cases. The solutions are expressed as Eqs. (A7)–(A11) in the appendix. The comparison between the analytical and the numerical orbitals is shown in Figs. 9–11.

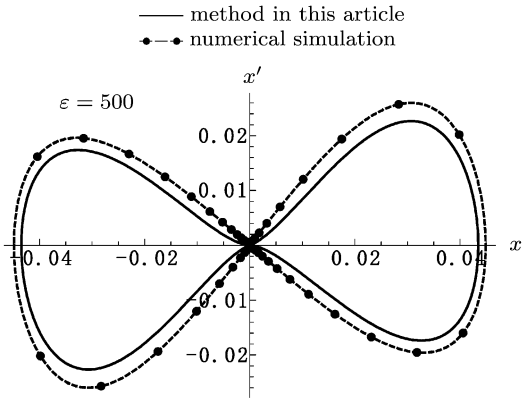


Fig. 9. Comparison of the homoclinic trajectory obtained using the present results with that obtained in the Runge–Kutta procedure.

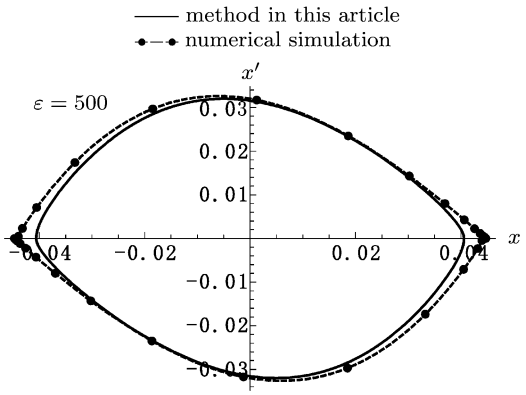


Fig. 10. Comparison of heteroclinic trajectories obtained using the present results with those obtained in the Runge–Kutta procedure.

Note that, when $c_1 > 0$, $c_3 < 0$, $c_2 = 0$, condition (33) of the heteroclinic orbital after the disturbance must be satisfied. And when $c_2^2 < 4c_1c_3$, $c_2c_3 \neq 0$, $c_1 < 0$, the perturbation parameter can be discussed in two different cases. When $\varepsilon = 1$, $\mu_1 = 0.1$, and $\mu_2 = 0.1$ as shown in Figs. 11(a) and 11(b), the perturbation is relatively small and has little effect on the orbitals. Simultaneously, the left-hand side or the right-hand side values of the global bifurcation point and the corresponding initial value can be derived. When $\varepsilon = 500$, as shown in Fig. 11(c), the perturbation is relatively large, the larger one of the homoclinic orbitals (the left one) breaks down, and the global bifurcations do not occur. All the left-hand side trajectories follow into the left centre. Thus we need to choose the global bifurcation of the smaller orbital to be calculated.

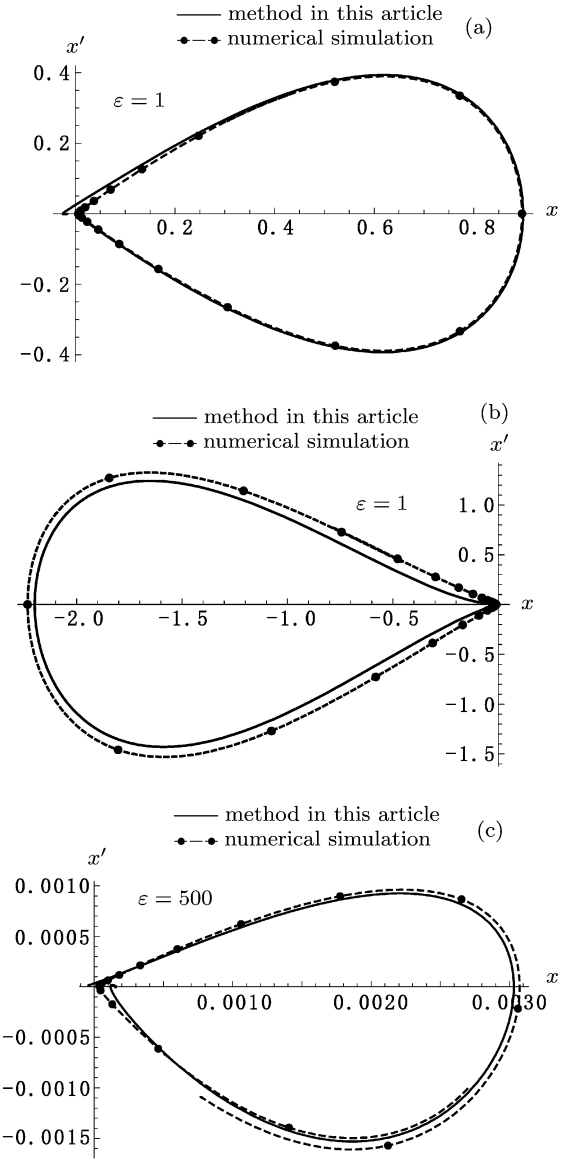


Fig. 11. Comparison of the homoclinic trajectory obtained using the present results with that obtained in the Runge–Kutta procedure: (a) bifurcation in the right-hand when $\varepsilon = 1$, (b) bifurcation in the left-hand when $\varepsilon = 1$, (c) bifurcation in the right-hand when $\varepsilon = 500$.

6. Nonautonomous system

Consider the periodic excitation oscillators $F = f\cos\omega t$,

$$\ddot{x} + c_1x + \varepsilon(c_2x^2 + c_3x^3 - f\cos\omega t) = 0. \qquad (39)$$

The solutions which will be considered are the periodic ones and those satisfying the special boundary value. Because the perturbation is too small, those analytical orbitals are the periodic ones that are close to the theoretical homoclinic or heteroclinic orbitals,

which are the separatrix cycles in the nonautonomous system (39). When $c_1 < 0$ and $c_3 > 0$, system (39) has two periodic orbitals on the interior of the separatrix cycles and one big orbital on the exterior of the separatrix cycles. When $c_1 > 0$ and $c_3 < 0$, system (39) has one periodic orbital on the interior of the separatrix cycles and no orbital on the exterior of the separatrix cycles. Those analytical progressive orbitals provide ideas to further improve the Melnikov method. Table 3 lists all the parameters involved in the calculation of the three cases. The solutions are expressed as Eqs. (A12)–(A17) in the appendix. The comparison between the analytical and the numerical orbitals is shown in Figs. 12–14.

Table 3. All parameters involved in the calculation of the three cases.

Case	$c_1 < 0$, $c_3 > 0$, $c_2 = 0$ $c_1 = -1$, $c_3 = 1$		$c_1 > 0$, $c_3 < 0$, $c_2 = 0$ $c_1 = -1$, $c_3 = -3$	$c_2^2 < 4c_1c_3$, $c_2c_3 \neq 0$, $c_1 < 0$ $c_1 = -1$, $c_2 = -1.5$, $c_3 = 1$	
Boundary-value	$\dot{x}(0) = 0$, $\lim_{t\to\infty} x(t) = 0$		$\lim_{t\to\pm\infty} x(t) = \pm\sqrt{-c_1/c_3}$, $\lim_{t\to\pm\infty} \dot{x}(t) = 0$ $\lim_{t\to\pm\infty} x(t) = \mp\sqrt{-c_1/c_3}$, $\lim_{t\to\pm\infty} \dot{x}(t) = 0$	$\dot{x}(0) = 0$, $\lim_{t\to\infty} x(t) = 0$	
Initial point	$(a, 0)$		(a, a_1)	$(a, 0)$	
ε	1		1	1	
F			$f = 0.01, \omega = 2$		
a	–1.40821	1.4252	–0.010003	–0.61026	1.62152
a_1			0.40938		

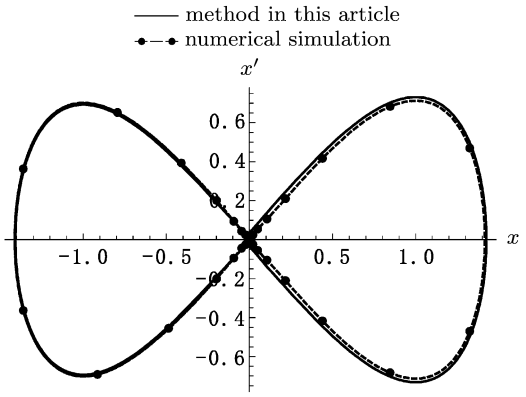


Fig. 12. Comparison of the trajectory obtained using the present results with that obtained in the Runge–Kutta procedure.

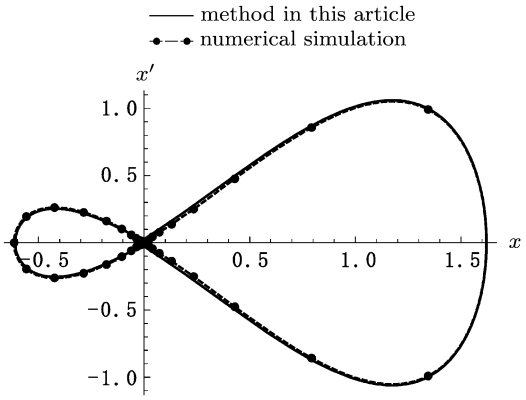


Fig. 14. Comparison of the trajectory obtained using the present results with that obtained in the Runge–Kutta procedure.

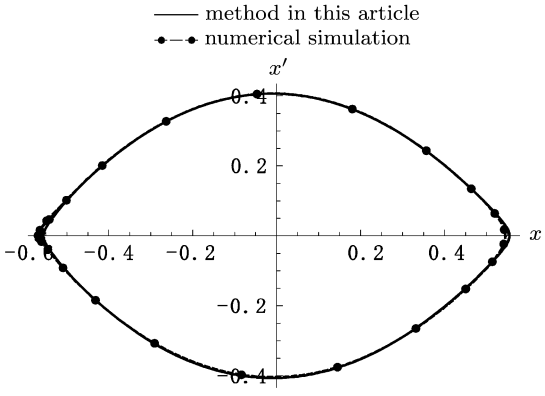


Fig. 13. Comparison of trajectories obtained using the present results with those obtained in the Runge–Kutta procedure.

7. Conclusion

The extended Padé approximant is utilized to solve the homoclinic and the heteroclinic orbitals in asymmetric nonlinear dynamical systems at origin. The methodology presented in this work is sufficiently general to be applicable to other types of nonlinear systems.

The general formulas of the homoclinic and the heteroclinic solutions are obtained in asymmetric nonlinear dynamical systems at origin with variable parameters. And simultaneously, the value of the global bifurcation is obtained. According to the specific examples, the asymmetric homoclinic orbitals remain as

they were when the disturbance parameter was relatively small; however, the larger orbital of the homoclinic orbitals breaks down, while the smaller one remains as it was when the disturbance parameter was relatively large.

In the process of analyzing the disturbance equation, on one hand, the condition that the initial point satisfied is proved by applying the Padé approximants, on the other hand, ε is directly involved in the differential equation no matter whether ε is small enough or not, and the solution is still valid.

Appendix A

$$\alpha_0 = a, \tag{A1}$$

$$\alpha_2 = a_2 - \frac{a_0(a_4a_6 - a_2a_8)}{a_4^2 - a_2a_6}, \tag{A2}$$

$$\alpha_4 = -\frac{-a_4^3 + 2a_2a_4a_6 - a_0a_6^2 - a_2^2a_8 + a_0a_4a_8}{a_4^2 - a_2a_6}, \tag{A3}$$

$$\beta_2 = -\frac{a_4a_6 - a_2a_8}{a_4^2 - a_2a_6}, \tag{A4}$$

$$\beta_4 = \frac{a_6^2 - a_4a_8}{a_4^2 - a_2a_6}, \tag{A5}$$

$$\alpha_1 = \alpha_3 = \beta_1 = \beta_3 = 0, \tag{A6}$$

$$\mathrm{PA}_4^{(1)+} = \frac{0.0434771 + 0.00682017t + 0.00682814t^2 + 0.000482872t^3 + 9.45263 \times 10^{-10}t^4}{1 + 0.156868t + 0.60218t^2 + 0.000227203t^3 + 0.0931039t^4}, \tag{A7}$$

$$\mathrm{PA}_4^{(2)+} = \frac{-0.00499391 + 0.030216t + 0.00936193t^2 + 0.00630774t^3 + 0.000260561t^4}{1 + 0.354326t + 0.394753t^2 + 0.0515497t^3 + 0.0243071t^4}, \tag{A8}$$

$$\mathrm{PA}_4^{(3)-} = \frac{-2.19849 + 0.282305t - 0.524079t^2 - 0.0658074t^3 - 3.32616 \times 10^{-6}t^4}{1 - 0.128409t + 1.05582t^2 - 0.174466t^3 + 0.264802t^4}, \tag{A9}$$

$$\mathrm{PA}_4^{(3)+} = \frac{0.899103 - 0.055033t - 0.0323178t^2 + 0.00359101t^3 - 3.21898 \times 10^{-12}t^4}{1 - 0.0612087t + 0.3178t^2 - 0.0189967t^3 + 0.0174852t^4}, \tag{A10}$$

$$\mathrm{PA}_4^{(3)+} = \frac{0.00303072 - 0.00111119t + 0.0000286311t^2 + 0.0000255242t^3 + 2.62532 \times 10^{-8}t^4}{1 - 0.366641t + 0.269424t^2 - 0.0291076t^3 + 0.0142056t^4}, \tag{A11}$$

$$\mathrm{PA}_4^{(1)-} = \frac{-1.40821 + 0.0371992t^2}{1 + 0.461558t^2 + 0.0251572t^4}, \tag{A12}$$

$$\mathrm{PA}_4^{(1)+} = \frac{1.4252 - 0.0715547t^2}{1 + 0.468897t^2 + 0.0218956t^4}, \tag{A13}$$

$$\mathrm{PA}_4^{(2)-} = \frac{-0.010003 - 0.412279t - 0.121037t^2 - 0.0227587t^3 - 0.0035827t^4}{1 + 0.290271t + 0.220693t^2 + 0.0579989t^3 + 0.0035827t^4}, \tag{A14}$$

$$\mathrm{PA}_4^{(2)+} = \frac{-0.010003 + 0.412279t - 0.121037t^2 + 0.0227587t^3 - 0.0035827t^4}{1 - 0.290271t + 0.220693t^2 - 0.0579989t^3 + 0.0035827t^4}, \tag{A15}$$

$$\mathrm{PA}_4^{(3)-} = \frac{-0.61026 + 0.0206299t^2}{1 + 0.288114t^2 + 0.0132494t^4}, \tag{A16}$$

$$\mathrm{PA}_4^{(3)+} = \frac{1.62152 - 0.0881909t^2}{1 + 0.86187t^2 + 0.0318905t^4}, \tag{A17}$$

References

[1] Guckenheimer J and Holmes P 1993 *Nonlinear Oscillations, Dynamical Systems and Bifurcations of Vector Fields* (New York: Springer)

[2] Wiggins S 1990 *Introduction to Applied Nonlinear Dynamical Systems and Chaos* (New York: Springer)

[3] Liu N and Guan Z H 2009 *Chin. Phys.* B **18** 1769

[4] Yang Z Q and Lu Q S 2006 *Chin. Phys.* **15** 518

[5] Chen X W 2002 *Chin. Phys.* **11** 441

[6] Chen J J and Yu S M 2009 *Acta Mech. Sin.* **58** 7525

[7] Wang Z, Li Y X, Hui X J and Lü L 2011 *Acta Mech. Sin.* **60** 010513

[8] Jiang B, Han X J and Bi Q S 2010 *Acta Mech. Sin.* **59** 8343

[9] Melnikov V K 1963 *Trans. Moscow Math.* **12** 1

[10] Emaci E, Vakakis A F, Andrianov I V and Mikhlin Y V 1997 *Nonlinear Dyn.* **13** 324

[11] Mikhlin Y V 2000 *J. Sound Vib.* **230** 971

[12] Manucharyan G V and Mikhlin Y V 2005 *Appl. Math. Mech.* **69** 39

[13] Zhang Q C, Wang W and Li W Y 2008 *Chin. Phys. Lett.* **25** 1905

[14] Zhang Q C, Wang W and He X J 2008 *Acta Mech. Sin.* **57** 5384

[15] Chen S S, Chen Y Y and Sze K Y 2009 *J. Sound Vib.* **322** 381

[16] Chen Y Y, Chen S S and Sze K Y 2009 *Acta Mech. Sin.* **25** 721

[17] Baker Jr G A and Gammel J L (edn.) 1970 *The Padé Approximant in Theoretical Physics* (New York: Academic Press)

[18] Baker Jr G A and Graves-Morris P R 1981 *Padé Approximants, part 2: Extension and Applications* (London: Addison–Wesley Publishing Company)

[19] Mikhlin Y V 1995 *J. Sound Vib.* **182** 577